Int. J. Electrochem. Sci., 11 (**2016**) 4865 – 4877, doi: 10.20964/2016.06.1

International Journal of
ELECTROCHEMICAL
SCIENCE
www.electrochemsci.org

Application of Pd-modified Nickel Foam Cathodes to the Process of Alkaline Water Electrolysis

Boguslaw Pierozynski[*], *Tomasz Mikolajczyk*

Department of Chemistry, Faculty of Environmental Management and Agriculture, University of Warmia and Mazury in Olsztyn, Plac Lodzki 4, 10-957 Olsztyn, Poland
[*]E-mail: bogpierozynski@yahoo.ca

Received: 21 February 2016 / *Accepted:* 17 March 2016 / *Published:* 1 May 2016

This work presents an investigation of hydrogen evolution reaction (HER) through the process of alkaline water electrolysis (AWE), performed by means of pure and palladium-modified nickel foam cathodes, and stainless steel anodes. Temperature-dependent kinetics of the HER were studied in 2 and 8 M KOH, over the temperature range: 20-60 ^{o}C through a.c. impedance spectroscopy and d.c. galvanostatic electrochemical experiments. The charge-transfer resistance, exchange current-density for the HER and other electrochemical parameters for examined catalyst samples were presented.

Keywords: Renewable energy; Alkaline water electrolysis; Pd-modified Ni foam; HER; Impedance spectroscopy

1. INTRODUCTION

With continuously increasing cost of electrical energy along with more and more demanding environmental regulations [1], hydrogen attracts significant attention as a future energy carrier. In addition, when combined with renewable electricity sources (such as solar and wind) hydrogen produced by alkaline or PEM (proton-exchange membrane) water electrolysis process can be considered as the only emission-free fuel of ultra-high purity. In combination with PEM fuel cells, H_2 could play a key role in creation of sustainable energy supply. At the moment, due to the high cost of electrolytic hydrogen production, as well as fuel cell stacks, implementation of this energy solution is typically limited to applications, where cost is of secondary importance (e.g. rescue teams, military operations, etc.). However, as significant progress on hydrogen energy-related research continues (including optimization of electrochemical methods for hydrogen generation and various means of its storage), it is predicted that hydrogen-powered fuel cells could significantly increase their presence both in the automotive market, as well as in stationary and mobile energy sectors right beyond the year 2020 [2-10].

Present work makes an extension to some former HER studies carried-out on catalytically active cathode materials (Pd-, Pt- and Ru-modified Ni foams), produced from this laboratory [11-13]. Here, pure and Pd-modified Ni foam HER cathodes were electrochemically evaluated in a small, laboratory-made alkaline water electrolyser unit.

2. EXPERIMENTAL

Aqueous, 2 and 8 M KOH solutions were prepared from potassium hydroxide pellets (Sigma-Ultra, KOH content: ≥85%, K_2CO_3 content: ≤2.0%). All solutions were made up using a Direct-Q3 UV ultra-pure water purification system from Millipore with 18.2 MΩ cm water resistivity. A PMMA (polymethyl methacrylate)-made, 750 cm^3 in volume, alkaline water electrolysis cell used in this work, is illustrated in Fig. 1.

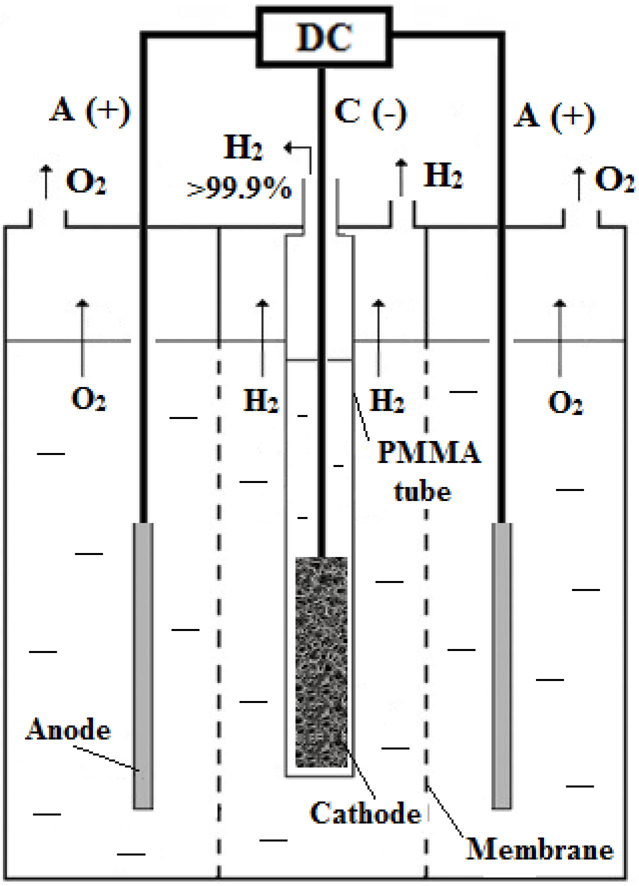

Figure 1. Schematic diagram of PMMA-made alkaline water electrolysis (AWE) cell; anode-to-anode and anode-to-cathode distances amount to 12 and 6 cm, correspondingly.

The cell is divided into three zones, where a middle part contains cathode (nickel foam-based cylindrical electrode, formed from 4×4 cm MTI nickel foam sheet), which is separated from two stainless steel-made (AISI 321: 5×4×0.1 cm) anodes by Zirfon Perl UTP 500 (polyphenylene sulphide/zirconium oxide) membranes delivered by Agfa-Gevaert N.V. In addition, a reversible Pd hydrogen electrode (RHE) was installed in the proximity of the cathode (working electrode), to act as a reference electrode for constant-potential HER impedance measurements. Prior to being installed in the electrolyser, Zirfon membranes were rinsed in ultra-pure Millipore water and soaked in 2 M KOH solution for 24 hours. Stainless steel anodes were polished with emery paper down to 2000 grade and de-greased with acetone. All procedures used for the preparation of Ni foam cathodes and the palladium RHE were as those described in our earlier works in Refs. [11-16].

Alkaline water electrolysis (AWE) experiments were carried-our under galvanostatic mode (at 0.5 and 1.0 A) by means of the Solartron 12,608 W Full Electrochemical System, consisting of 1260 frequency response analyzer (FRA) and 1287 electrochemical interface (EI). All information on the performed a.c. impedance measurements (including details of the fitting procedure) could be found in Ref. [11].

3. RESULTS AND DISCUSSION

3.1. Galvanostatic AWE experiments on pure and Pd-modified Ni foam materials in 2 and 8 M KOH solutions

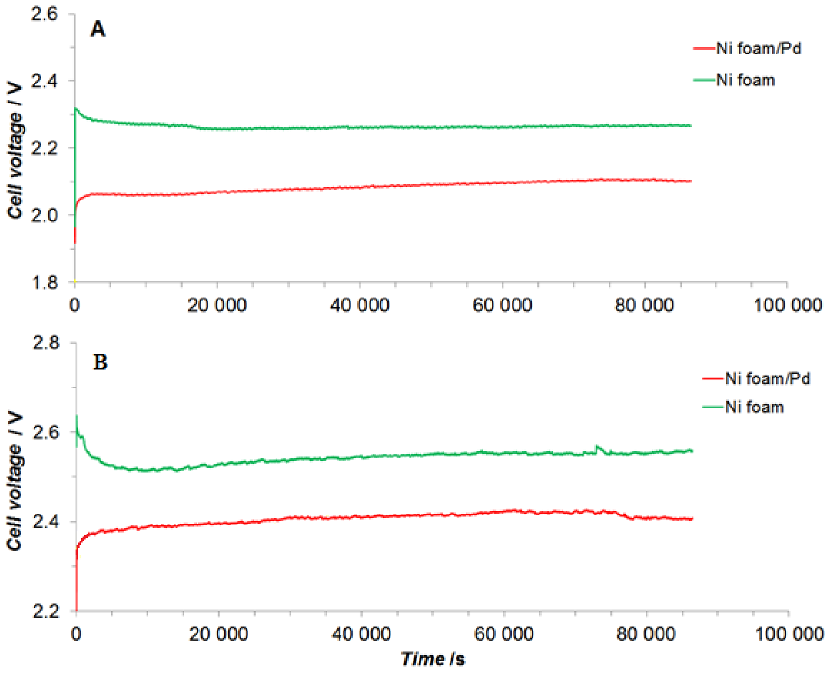

Figure 2. Cell voltage as a function of time over a 24-hour period, examined in PMMA-made AWE cell with Zirfon® electrode separating membrane at 50 ºC in 2 M KOH for current of 0.5 A (j_c= 2 mA cm^{-2}) (**A**) and 1.0 A (j_c= 4 mA cm^{-2}) (**B**).

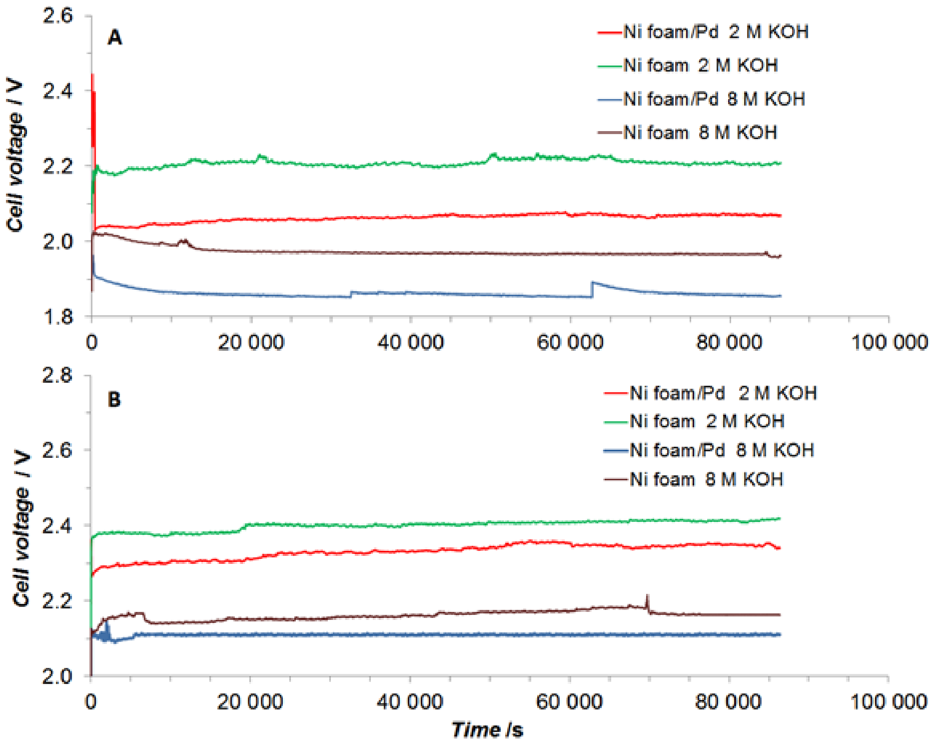

Figure 3. Cell voltage as a function of time over a 24-hour period, examined at 70 ºC in 2 & 8 M KOH (other details as in Figure 2 above).

Fig. 2 shows the results of galvanostatic AWE tests carried-out over the period of 24 hours for pure and Pd-modified Ni foam cathodes in 2 M KOH (at 50 ºC) for two cathodic current-densities of j_c= 2 (Fig. 2A) and 4 (Fig. 2B) mA cm^{-2}. Average cell voltages at the current-density of 2 mA cm^{-2} for Ni foam and the Pd-modified Ni cathodes were 2.28 and 2.06 V, correspondingly, where voltage fluctuation range for both electrodes came to about ± 35 mV. Furthermore, for the current-density of 4 mA cm^{-2} (Fig. 2B) an increase of the average cell voltage was recorded: by 220 and 300 mV for pure and the Pd-modified foam electrodes, respectively. However, the voltage oscillation for both electrodes stayed at the same level.

Fig. 3 presents the cell voltage as a function of time over a 24-hour period, recorded for pure and the Pd-modified Ni foam cathodes, but in 2 & 8 M KOH at 70 ºC for two current-densities of j_c= 2 (Fig. 3A) and 4 (Fig. 3B) mA cm^{-2}. Here, average cell voltages at the current-density of 2 mA cm^{-2} for pure and the Pd-modified cathodes were 2.20 and 2.05 V (2 M KOH), and 1.97 and 1.87 V (8 M KOH), correspondingly. The voltage fluctuation range for all electrodes was around ± 25 mV in 2 M KOH and ± 30 mV in 8 M KOH. Then, for the cathodic current-density of 4 mA cm^{-2} (Fig. 3B) the average cell voltages for Ni foam and the Pd-modified cathodes increased by *ca*. 200 and 260 mV (2 M KOH), and by 190 and 240 mV (8 M KOH), respectively. Analogous, long-term galvanostatic AWE tests (including those run on zero-gap electrode assemblies) were reported by other authors (see Refs. [17-21]). However, the results presented in these works for surface-modified HER catalysts were typically recorded with respect to initial (unmodified), geometrical values of electrode surface area (contrast to the results given in this article, where catalyst-modified surface area of Ni foam - very large to start with and difficult to be properly estimated, was approximated through the appropriate C_{dl} measurements). Thus, in case where no straight current-density comparisons could be made, making direct analogies between the cell voltages obtained in this work and those of other stated articles [17-21] would not be very meaningful.

3.2. Temperature dependent a.c. impedance behaviour of the HER on pure and Pd-modified Ni foam cathodes

The results of a.c. impedance measurements conducted directly in the alkaline water electrolyser on pure and the Pd-modified nickel foam cathodes are presented in Figs. 4 and 5, and Tables 1 and 2 for 2 M and 8 M KOH solutions, respectively.

Table 1. Electrochemical parameters for the HER on cathodically activated, pure and Pd-modified Ni foam electrodes in contact with 2 M KOH, studied over the temperature range 20-60 ºC.

***E*/ mV**	**Pure Ni foam in 2 M KOH**				
	20 °C	30 °C	40 °C	50 °C	60 °C
	R_{ct}/ Ω g				
-50	12.208 ± 0.140	5.313 ± 0.115	3.858 ± 0.057	2.375 ± 0.031	1.907 ± 0.066
-100	6.664 ± 0.072	3.293 ± 0.044	2.354 ± 0.029	2.022 ± 0.019	0.948 ± 0.020
-150	2.010 ± 0.017	1.154 ± 0.009	0.974 ± 0.008	0.960 ± 0.008	0.408 ± 0.007
-200	0.638 ± 0.005	0.563 ± 0.007	0.397 ± 0.003	0.380 ± 0.004	0.199 ± 0.003
-250	0.299 ± 0.003	0.275 ± 0.003	0.210 ± 0.002	0.184 ± 0.003	0.127 ± 0.004
-300	0.194 ± 0.002	0.150 ± 0.002	0.135 ± 0.002	0.109 ± 0.002	0.093 ± 0.003
-400	0.103 ± 0.002	0.067 ± 0.002	0.071 ± 0.002	0.053 ± 0.002	0.041 ± 0.002
C_{dl}/ μF g^{-1} $s^{\varphi 1-1}$					
-50	8,321 ± 504	18,184 ± 486	18,559 ± 470	19,896 ± 605	25,095 ± 3,670
-100	6,545 ± 244	13,084 ± 305	14,809 ± 473	15,355 ± 423	18,688 ± 1,092
-150	6,799 ± 295	10,360 ± 377	10,886 ± 390	12,163 ± 373	12,454 ± 1,034
-200	5,754 ± 192	7,983 ± 375	7,463 ± 462	7,608 ± 475	8,409 ± 1,020
-250	5,859 ± 444	5,732 ± 717	5,540 ± 513	6,609 ± 414	5,738 ± 384
-300	4,697 ± 508	4,729 ± 704	4,899 ± 631	6,440 ± 518	4,433 ± 307
-400	4,134 ± 732	3,736 ± 584	3,203 ± 737	2,764 ± 841	2,822 ± 329

Pd-modified Ni foam in 2 M KOH					
R_{ct}/ Ω g					
-50	1.254 ± 0.007	1.025 ± 0.022	0.812 ± 0.009	0.496 ± 0.007	0.394 ± 0.004
-100	0.701 ± 0.004	0.681 ± 0.005	0.575 ± 0.007	0.381 ± 0.004	0.328 ± 0.005
-150	0.428 ± 0.004	0.425 ± 0.005	0.366 ± 0.002	0.267 ± 0.004	0.244 ± 0.004
-200	0.265 ± 0.002	0.255 ± 0.001	0.244 ± 0.003	0.181 ± 0.003	0.176 ± 0.003
-250	0.176 ± 0.003	0.155 ± 0.001	0.144 ± 0.002	0.131 ± 0.003	0.118 ± 0.002
-300	0.124 ± 0.002	0.105 ± 0.001	0.090 ± 0.002	0.096 ± 0.001	0.077 ± 0.002
-400	0.052 ± 0.001	0.053 ± 0.001	0.053 ± 0.001	0.047 ± 0.002	0.036 ± 0.001
C_{dl}/ μF g^{-1} s$^{\varphi 1-1}$					
-50	101,770 ± 804	101,120 ± 2,993	130,021 ± 2,513	139,138 ± 4,344	165,813 ± 4,352
-100	103,332 ± 1,219	110,063 ± 1,818	123,516 ± 3,228	129,696 ± 3,723	154,245 ± 5,138
-150	113,161 ± 2,667	99,659 ± 2,653	111,113 ± 1,520	145,691 ± 6,274	163,423 ± 6,691
-200	110,639 ± 1,940	95,957 ± 2,246	127,213 ± 5,337	146,609 ± 7,436	174,609 ± 8,243
-250	105,950 ± 3,928	84,307 ± 4,021	121,952 ± 4,082	161,152 ± 14,138	188,857 ± 12,983
-300	92,193 ± 4,800	80,889 ± 4,512	132,230 ± 9,253	162,798 ± 11,520	194,536 ± 13,573
-400	59,475 ± 4,463	60,568 ± 4,943	150,727 ± 18,937	121,541 ± 16,363	173,588 ± 20,023

Table 2. Electrochemical parameters for the HER on cathodically activated, pure and Pd-modified Ni foam electrodes in contact with 8 M KOH, studied over the temperature range 20-60 ºC.

***E*/ mV**	**Pure Ni foam in 8 M KOH**				
	20 °C	30 °C	40 °C	50 °C	60 °C
	R_{ct}/ Ω g				
-50	8.075 ± 0.050	6.664 ± 0.095	3.558 ± 0.020	2.825 ± 0.026	2.609 ± 0.025
-100	2.081 ± 0.013	1.703 ± 0.017	0.939 ± 0.006	0.678 ± 0.005	0.523 ± 0.010
-150	0.744 ± 0.004	0.554 ± 0.005	0.448 ± 0.003	0.379 ± 0.003	0.362 ± 0.002
-200	0.322 ± 0.003	0.228 ± 0.003	0.185 ± 0.002	0.180 ± 0.002	0.122 ± 0.002
-250	0.232 ± 0.002	0.176 ± 0.003	0.139 ± 0.001	0.111 ± 0.002	0.089 ± 0.002
-300	0.155 ± 0.002	0.111 ± 0.002	0.066 ± 0.001	0.053 ± 0.001	0.042 ± 0.001

-400	0.062 ± 0.001	0.043 ± 0.001	0.040 ± 0.001	0.034 ± 0.001	0.032 ± 0.001
C_{dl}/ μF g^{-1} s$^{\varphi1-1}$					
-50	8,513 ± 281	17,396 ± 352	20,102 ± 192	16,100 ± 386	26,280 ± 435
-100	7,025 ± 162	13,719 ± 454	12,331 ± 345	13,808 ± 454	16,132 ± 465
-150	6,119 ± 266	9,256 ± 445	9,123 ± 373	11,119 ± 321	12,451 ± 415
-200	6,139 ± 328	6,929 ± 472	7,437 ± 402	7,955 ± 173	8,440 ± 235
-250	5,228 ± 367	6,222 ± 358	5,435 ± 396	7,030 ± 380	6,612 ± 880
-300	4,063 ± 336	4,430 ± 471	4,666 ± 876	3,400 ± 242	3,892 ± 356
-400	3,599 ± 347	3,622 ± 369	3,598 ± 441	2,525 ± 470	3,652 ± 691
Pd-modified Ni foam in 8 M KOH					
R_{ct}/ Ω g					
-50	0.814 ± 0.008	0.778 ± 0.005	0.631 ± 0.005	0.403 ± 0.004	0.286 ± 0.002
-100	0.636 ± 0.003	0.532 ± 0.006	0.435 ± 0.005	0.306 ± 0.002	0.264 ± 0.002
-150	0.397 ± 0.003	0.267 ± 0.002	0.220 ± 0.002	0.201 ± 0.003	0.121 ± 0.001
-200	0.217 ± 0.001	0.129 ± 0.001	0.123 ± 0.001	0.126 ± 0.001	0.085 ± 0.001
-250	0.127 ± 0.001	0.079 ± 0.001	0.074 ± 0.001	0.070 ± 0.001	0.065 ± 0.002
-300	0.077 ± 0.001	0.067 ± 0.001	0.051 ± 0.002	0.048 ± 0.001	0.040 ± 0.001
-400	0.040 ± 0.001	0.034 ± 0.001	0.036 ± 0.001	0.035 ± 0.001	0.031 ± 0.001
C_{dl}/ μF g^{-1} s$^{\varphi1-1}$					
-50	95,330 ± 5,717	131,293 ± 11,325	169,925 ± 7,474	199,554 ± 4,868	226,679 ± 4,941
-100	94,384 ± 4,293	141,866 ± 3,514	146,430 ± 8,407	155,336 ± 2,805	157,527 ± 2,345
-150	89,780 ± 7,514	128,868 ± 5,688	132,654 ± 3,225	139,254 ± 2,625	149,820 ± 7,755
-200	81,120 ± 1,805	124,200 ± 5,474	131,000 ± 4,250	133,363 ± 3,005	138,507 ± 5,388
-250	76,550 ± 944	115,252 ± 6,473	120,301 ± 4,854	124,154 ± 1,234	129,968 ± 4,584
-300	68,539 ± 989	88,545 ± 1,089	111,234 ± 3,684	112,352 ± 1,173	109,234 ± 14,890
-400	79,698 ± 2,032	79,679 ± 8,320	121,720 ± 2,620	103,713 ± 11,547	117,236 ± 13,785

At room temperature (20 ºC), all recorded impedance results displayed two “depressed” partial semicircles, at all examined potentials in the investigated frequency range. There, the high-frequency semicircle (practically overpotential independent) corresponds to the porosity of the electrode, whereas the low-frequency response is related to the kinetics of the hydrogen evolution reaction [22-25]. However, as the high frequency semicircles were not well-pronounced at higher temperatures, the porosity response was not included in the impedance fittings/calculations (all fittings were performed with a simple CPE-modified Randles equivalent circuit model, see later Fig. 6).

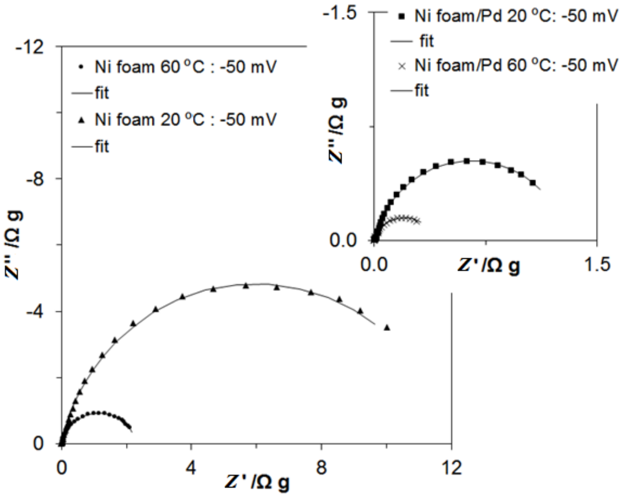

Figure 4. Complex-plane impedance plots for the HER on pure and Pd-modified (inset) Ni foam electrodes in contact with 2 M KOH, recorded at 20 and 60 ºC for -50 mV (vs. RHE). Solid lines correspond to representation of the data according to the equivalent circuit shown in Figure 6.

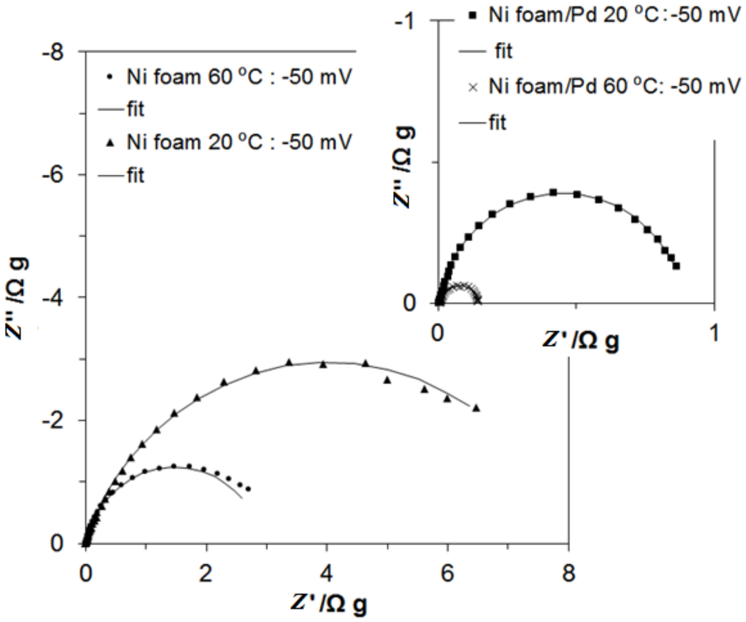

Figure 5. Complex-plane impedance plots for the HER on pure and Pd-modified (inset) Ni foam electrodes in contact with 8 M KOH, recorded at 20 and 60 ºC for -50 mV (other details as in Figure 5 above).

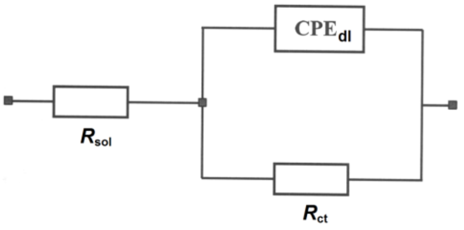

Figure 6. An equivalent circuit used for fitting the HER impedance data for pure and Pd-modified Ni foam electrodes, obtained in 2 and 8 M KOH. The circuit combines a constant phase element (CPE) for distributed capacitance; R_{ct} and C_{dl} (as CPE$_{dl}$) elements correspond to the HER charge-transfer resistance and double-layer capacitance components, and R_{sol} is solution resistance.

Thus, both Ni foam-based electrodes exhibited single, “depressed” semicircles (a single-step charge-transfer reaction) at all potentials, at the temperature range of 20-60 ºC in both electrolyte solutions (see examples of the recorded Nyquist impedance plots in Figs. 4 and 5). Moreover, comparison of Faradaic reaction resistance (R_{ct}) and double-layer capacitance (C_{dl}) parameters for the HER at the examined Ni foam-based cathodes (derived by means of an equivalent circuit illustrated in Fig. 6) is shown in Tables 1 and 2. The CPE element was used in the circuit in order to account for the so-called “capacitance dispersion” effect [26, 27].

Hence, at 20 ºC and 2 M KOH for cathodically activated Ni foam and Pd-modified foam electrodes the recorded R_{ct} parameter diminished from 12.208 and 1.254 Ω g at -50 mV to 0.103, and 0.052 Ω g at the potential of -400 mV vs. RHE, correspondingly. A radical reduction of the R_{ct} parameter (by *ca*. 9.7 and 2.0× at −50, and −400 mV, respectively) results from the catalytic nature of nanocrystalline palladium deposit. Interestingly, these surface-deposited Pd nanoparticles (*ca*. 10 nm and 0.1 wt. % Pd [11, 12]) caused a significant enhancement of electrochemically available surface area, as compared to that of the nickel foam baseline cathode. Thus, for the Pd-activated Ni foam, the recorded values of the C_{dl} parameter at −50 mV came to 101,770 μF g^{-1} $s^{\varphi 1-1}$, which is *ca*. 12.2× greater than the C_{dl} derived for the baseline Ni foam cathode: 8,321 μF g^{-1} $s^{\varphi 1-1}$ (Table 1). Now, when these capacitance values (recorded for the electrode weight of 0.560 g) are referred to that commonly used value of 20 μF cm^{-2} in literature for smooth and homogeneous surfaces [28, 29], electrochemically active surface area of examined cathodes could be estimated at 233 cm^2 (pure Ni foam) and 2,850 cm^2 for the palladium-modified foam electrode. Furthermore, a considerable reduction of the C_{dl} parameter with increasing overpotential is an outcome of partial blocking of electrochemically active electrode surface by newly formed H_2 micro-bubbles within highly porous Ni foam entity.

Table 1 also shows the temperature dependence of the R_{ct} and C_{dl} parameters, investigated over the temperature range: 20–60 °C (2 M KOH). Hence, for two temperature extremes, namely 20 and 60 °C, the recorded charge-transfer resistance at −50 mV exhibited significant reduction from 12.208 to 1.907 Ω g (6.4×) for unmodified Ni foam and from 1.254 to 0.394 (3.2×) for the Pd-modified cathode. Similarly, at the cathodic overpotential of 400 mV, the respective R_{ct} parameter values ranged from 0.103 to 0.041 Ω g (2.5×) and from 0.052 to 0.036 Ω g (1.4×), correspondingly. Additionally, upon increasing temperature, the C_{dl} parameter recorded at individual overpotentials kept slowly rising (see Table 1 again). This phenomenon could be explained in terms of additional access to the catalyst surface, gained within the porous electrode structure at higher temperatures (enhanced process of hydrogen bubble removal accompanied by increased conductivity of the electrolyte).

In 8 M KOH solution, the recorded R_{ct} and C_{dl} parameter values (see Table 2) followed the same trend as those obtained in 2 M KOH. Hence, the charge transfer resistance R_{ct} kept decreasing upon rising temperature and cathodic overpotential. It should also be noticed that the R_{ct} values derived in 8 M KOH solution were generally smaller than those recorded in 2 M potassium hydroxide electrolyte (compare the corresponding results in Table 1 with those of Table 2). Again, at fixed temperature the C_{dl} parameter exhibited significant reduction with increasing overpotential, while temperature increase for the set overpotential resulted in significantly rising double-layer capacitance values (Table 2). Finally, dimensionless φ_1 parameter [11] of the CPE circuit (see Fig. 6 and Tables 1, and 2), varied between 0.79–0.98 (2 M KOH) and 0.81–0.95 (8 M KOH), respectively.

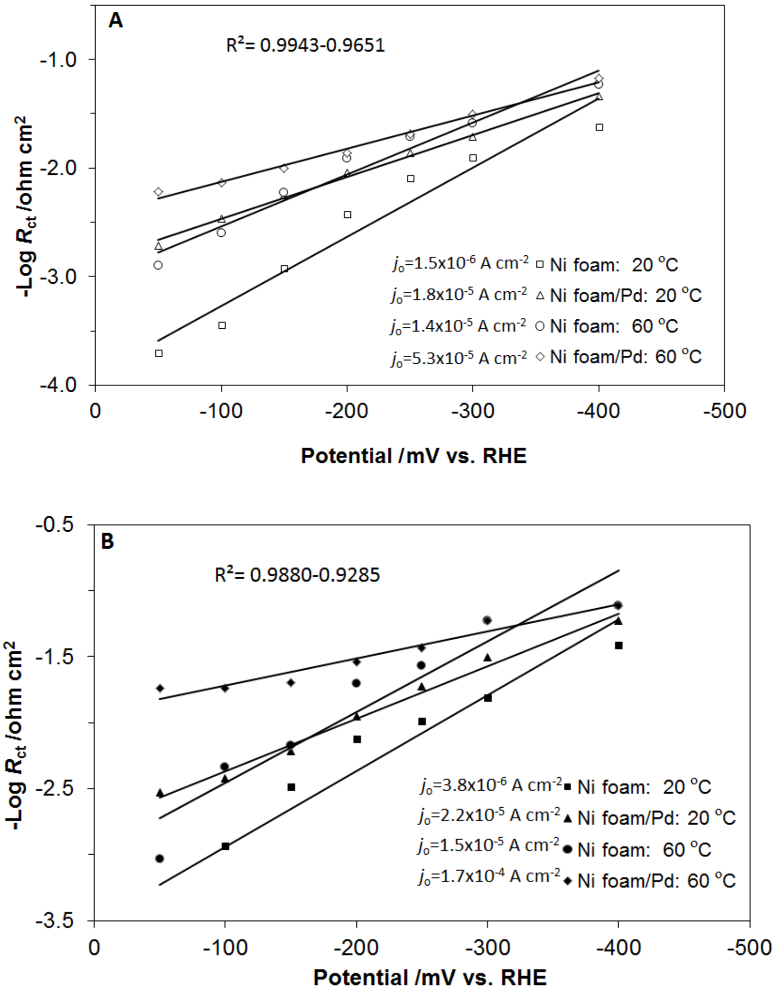

Figure 7. Linear plots of −log R_{ct} in function of potential (vs RHE), obtained for the HER performed on pure and Pd-modified Ni foam electrodes in 2 (**A**) and 8 (**B**) M KOH solutions, recorded at 20 and 60 °C. Symbols represent experimental results and lines are data fits.

Furthermore, a graph of –log R_{ct} vs. overpotential (see Figs. 7AB) showed relatively good linear dependence for both examined electrodes and electrolyte solutions, over the studied overpotential range. The exchange current-densities (j_0) for the HER were calculated through the Butler-Volmer equation (see e.g. Ref. [14]), based on the relation between the j_0 and the R_{ct} parameters for overpotential approaching zero [30-32]. Hence, the calculated values of the j_0 parameter came to 1.5×10^{-6} A cm^{-2} (at 20 °C) and 1.4×10^{-5} A cm^{-2} (at 60 °C) for the unmodified Ni foam in 2 M KOH. However, significantly increased j_0 values, namely: 1.8×10^{-5} A cm^{-2} (at 20 °C) and 5.3×10^{-5} A cm^{-2} (at 60 °C) were recorded for the Pd-modified nickel foam catalyst material in this electrolyte (see Fig. 7A for details). On the other hand, the calculated HER exchange current-densities for 8 M KOH were significantly increased, namely by 2.5× (Ni foam at 20 ^{o}C), 1.2× (Ni foam/Pd at 20 ^{o}C), 1.1× (Ni foam at 60 ^{o}C) and 3.2× (Ni foam/Pd at 60 ^{o}C).

It should be stressed that the HER exchange current-density values for the Pd-activated nickel foam (derived at 20 °C) presented in this paper compare fairly well with the corresponding j_0s values recorded for 3D porous Ni-based electrode entities: (1-6)$\times10^{-5}$ A cm^{-2} [22, 23, 33]. Furthermore, in some HER articles [25, 34] electrochemical results for catalytically-modified cathodes are presented with respect to unmodified (initial) geometric surface area of a baseline material. Hence, such-calculated exchange current-densities: (1.0-9.5)$\times10^{-3}$ A cm^{-2} come close to those quoted for platinum electrodes. Therefore, for a spongy-type entity such as Ni foam electrode, some electrochemical results might suitably be presented as per electrode mass. Otherwise, the results should be given with respect to the C_{dl}-estimated, electrochemically active surface area of the catalyst-modified electrode.

Table 3. Apparent activation energy parameters for the HER, obtained on cathodically activated, pure and Pd-modified Ni foam electrodes in contact with 2 and 8 M KOH solutions, studied over the temperature range 20-60 ºC.

***E*/ mV**	***E*$_A$/ kJ mol^{-1}**			
	Pure Ni foam 2 M KOH	Pd-modified Ni foam 2 M KOH	Pure Ni foam 8 M KOH	Pd-modified Ni foam 8 M KOH
-100	35.6	16.9	29.9	18.7
-400	16.3	6.7	12.9	3.9

In addition, Figs. 8AB present −log R_{ct} versus T^{-1} Arrhenius-type plots, constructed based on the R_{ct}=f(T) impedance results and presented for the overpotentials of 100 and 400 mV (vs. RHE). Table 3 illustrates electrochemical energies of activation (E_A) [kJ mol^{-1}] for the HER at the corresponding overpotential values, calculated for both Ni foam-based cathodes and two examined electrolytes. Hence, for the palladium-modified Ni foam electrode examined in 8 M KOH activation energies came to 18.7 and 3.9 kJ mol^{-1} at -100 and -400 mV, respectively (compare with 34.3 and 10.2 kJ mol^{-1} recorded on Pd-activated Ni foam in 0.1 M NaOH, at the respective values of the cathodic overpotential [12]).

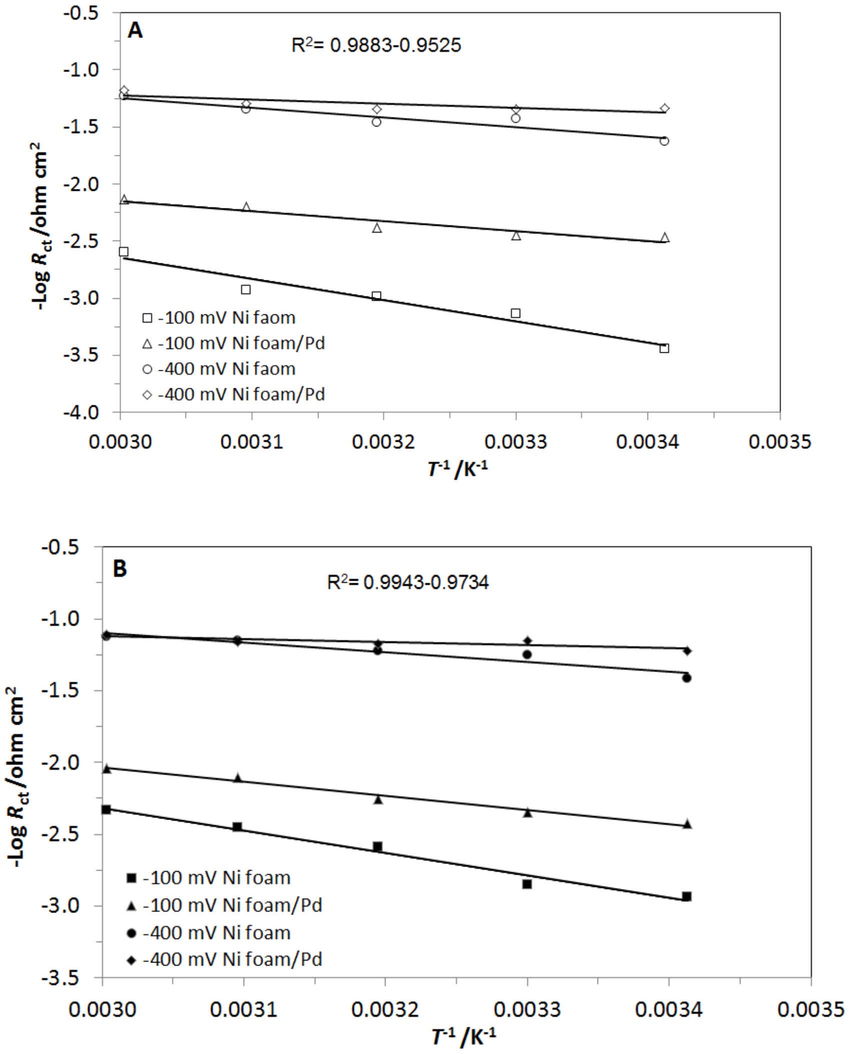

Figure 8. Linear plots of −log R_{ct} versus T^{-1} for the HER preformed on pure and Pd-modified Ni foam electrodes in 2 (**A**) and 8 (**B**) M KOH solutions, at the stated overpotential values.

4. CONCLUSIONS

A key objective of this work was to verify the stability of prepared cathode composite materials by conducting extended alkaline water electrolysis experiments. The results presented in this work proved that palladium-modified Ni foam would be well-suited as a new type of cathode for alkaline water electrolysers, not only because of its long term catalytic stability, but also thanks to its exceptional corrosion resistance at high pH values and large, specific electrochemically active surface area. Furthermore, Ni foam-based cathodes would be less expensive and complicated to produce on a commercial scale, as compared to typical 3D porous type, nonhomogeneous Ni-based electrodes.

Further work should cover extended to several months AWE experiments carried-out on Pd-activated nickel foam cathodes in 8 M KOH solution. In addition, complementary efforts would involve optimization of electrolyser's anode system (elimination of stainless steel anodes) along with inter-electrode distances for minimized voltage parameter [1, 7].

References

1. K. Zeng and D. Zhang, *Prog. Energy Combust. Sci.*, 36 (2010) 307.
2. K. Christopher and R. Dimitrios, *Energy Environ. Sci.*, 5 (2012) 6640.
3. S. Vengatesan, S. Santhi, S. Jeevanantham and G. Sozhan, *J. Power Sources*, 284 (2015) 361.
4. M. Momirlan and T.N. Veziroglu, *Int. J. Hydrogen Energy*, 30 (2005) 795.
5. R. Solmaz, *Int. J. Hydrogen Energy*, 38 (2013) 2251.
6. A. Manabe, M. Kashiwase, T. Hashimoto, T. Hayashida, A. Kato, K. Hirao, I. Shimomura and I. Nagashima, *Electrochim. Acta*, 100 (2013) 249.
7. M.M. Rashid, M.K.A. Mesfer, H. Naseem and M. Danish, *IJEAT*, 4 (2015) 80.
8. S.A. Grigoriev, V.I. Porembsky and V.N. Fateev, *Int. J. Hydrogen Energy*, 31 (2006) 171.
9. M. Granovskii, I. Dincer and M.A. Rosen, *J. Power Sources*, 157 (2006) 411.
10. W. Kreuter and H. Hofmann, *Int. J. Hydrogen Energy*, 23 (1998) 661.
11. B. Pierozynski, T. Mikolajczyk and I.M. Kowalski, *J. Power Sources*, 271 (2014) 231.
12. B. Pierozynski and T. Mikolajczyk, *Electrocatalysis*, 6 (2015) 51.
13. B. Pierozynski and T. Mikolajczyk, *Electrocatalysis*, DOI 10.1007/s12678-015-0290-x.
14. B. Pierozynski and L. Smoczynski, *J. Electrochem. Soc.*, 156(9) (2009) B1045.
15. B. Pierozynski, *Int. J. Electrochem. Sci*., 6 (2011) 63.
16. B. Pierozynski, *Int. J. Hydrogen Energy*, 38 (2013) 7733.
17. Ph. Vermeiren, J.P. Moreels, A. Claes and H. Beckers, *Int. J. Hydrogen Energy*, 34 (2009) 9305.
18. D. Pletcher, X. Li and S. Wang, *Int. J. Hydrogen Energy*, 37 (2012) 7429.
19. D. Pletcher and X. Li, *Int. J. Hydrogen Energy*, 36 (2011) 15089.
20. M.P.M. Kaninski, S.M. Miulovic, G.S. Tasic, A.D. Maksic and V.M. Nikolic, *Int. J. Hydrogen Energy*, 36 (2011) 5227.
21. X. Qian, T. Hang, S. Shanmugam and M. Li, *ACS Appl. Mater. Interfaces*, 7 (2015) 15716.
22. M.A. Dominguez-Crespo, E. Ramirez-Meneses, A.M. Torres-Huerta, V. Garibay-Febles and K. Philippot, *Int. J. Hydrogen Energy*, 37 (2012) 4798.
23. M.A. Dominguez-Crespo, A.M. Torres-Huerta, B. Brachetti-Sibaja and A. Flores-Vela, *Int. J. Hydrogen Energy*, 36 (2011) 135.
24. R. Solmaz, A. Gundogdu, A. Doner and G. Kardas, *Int. J. Hydrogen Energy*, 37 (2012) 8917.
25. C. Hitz and A. Lasia, *J. Electroanal. Chem.*, 500 (2001) 213.
26. T. Pajkossy, *J. Electroanal. Chem.*, 364 (1994) 111.
27. B.E. Conway and B. Pierozynski, *J. Electroanal. Chem*., 622 (2008) 10.
28. A. Lasia and A. Rami, *J. Appl. Electrochem.*, 22 (1992) 376.
29. L. Chen and A. Lasia, *J. Electrochem. Soc*., 138 (1991) 3321.
30. J.G. Highfield, E. Claude and K. Oguro, *Electrochim. Acta*, 44 (1999) 2805.
31. R.K. Shervedani and A.R. Madram, *Electrochim. Acta*, 53 (2007) 426.
32. S. Martinez, M. Metikos-Hukovic and L. Valek, *J. Mol. Catal. A Chem*., 245 (2006) 114.
33. J.M. Jaksic, M.V. Vojnovic and N.V. Krstajic, *Electrochim. Acta*, 45 (2000) 4151.
34. V.M. Nikolic, S.Lj. Maslovara, G.S. Tasic, T.P. Brdaric, P.Z. Lausevic, B.B. Radak and M.P.M. Kaninski, *Appl. Catal. B-Environ.*, 179 (2015) 88.